

The effect of homogenization on the recrystallization of an Al-Mn-Mg alloy sheet

M. AGHAIE-KHAFRI

Materials Division, Faculty of Mechanical Engineering, K.N. Toosi University of Technology, Pasdaran Street, Amir Ebrahimi street, Adjacent to Boostan 2, No. 6, Postal Code: 1664664313, Tehran, Iran
E-mail: maghaei@kntu.ac.ir

The present study examines the effect of homogenization of the roll-cast material on the microstructure and ductility of an Al-Mn-Mg alloy sheet. The phenomenon of recrystallization and the effect of precipitation and second phase particles have been investigated in cold rolled sheets by means of differential scanning calorimetry (DSC), electrical conductivity measurement and image analysis. It appears that recrystallization characteristics in different homogenization conditions are important parameters that control the grain sizes and consequently the ductility of the homogenized sheets. It is believed that homogenization promotes normal discontinuous recrystallization and subsequent grain coarsening mainly due to the elimination of precipitation interaction and the coarsening of the second phase particles.

© 2005 Springer Science + Business Media, Inc.

1. Introduction

AA3xxx alloys which are generally used in the transportation, food and beverage, and packaging industries are attractive materials due to the fact that they can provide a suitable combination of strength and formability. The principal strengthening agents in AA3xxx alloys are primary and secondary constituent particles. These particles are capable of stabilizing a fine grain structure or suitable texture which can develop interesting combinations of strength and formability.

The most striking observation with regard to formability among the Al-Mn-Mg alloys is the poor performance of the strip-cast materials without any homogenization heat treatment [1]. Homogenization of the as-cast material brings about changes in size, shape and distribution of primary and secondary precipitates which in turn, impact the subsequent processability and influence the final product properties. Numerous investigations have been done on the influence of constituent particles, including fine dispersoids and large primary particles on the recrystallization, texture and mechanical behavior of the aluminum alloys [2–4]. It is well established that the finely dispersed particles inhibit recrystallization while large particles promote recrystallization [5, 6].

Differential scanning calorimetry is a useful technique for the study of phase transformations and has been widely applied to study precipitation and the interaction between precipitation and recrystallization in aluminum alloys [7, 8]. DSC has the advantages of (1) analyzing comparatively large volumes of material, (2) quantitative data output, and (3) minimal time and sample preparation [9, 10].

The present investigation examines the influence of preheating of the roll-cast Al-Mn-Mg alloy on the microstructure of subsequently rolled sheets by means of calorimetry and electrical conductivity measurements and microstructural evaluation.

2. Experimental procedures

2.1. Materials and processing

The material used in this investigation was an Al-Mn-Mg alloy containing (in wt.%) 0.32 Fe, 0.21 Si, 0.32 Mn, 0.34 Mg with minor constituents of, 0.01Cu, 0.01Zn and 0.02Ti. It was roll-cast to 8 mm thickness before receiving different thermomechanical treatments. Some of the strips were cold rolled to a final thickness of 1 mm without prior homogenization, and some others were homogenized and then cold rolled to the same final thickness. In both conditions the rolled sheets were annealed in the temperature range of 270–450°C. Homogenized and unhomogenized conditions are referred to hereafter as “H” and “U” respectively.

2.2. DSC measurements

Samples for DSC measurements were in a disc shape, 5 mm diameter, sparked out of the cast strips and the rolled sheets. The calorimetric measurements were performed using a DSC apparatus. Runs were carried out at heating rate 5°C/min and under dynamic argon atmosphere. High purity aluminum was used as reference. To check whether precipitation occurred during homogenization, the electrical conductivity was measured.

2.3. Microstructural measurements

The size and distribution of the particles were determined on the basis of the image analysis of the TEM micrographs. An image analysis software, Clemex, were used for image processing. The software uses the binarization processing, that is each pixel has an intensity value ranging from 0–250 and a specific range of pixels are assigned binary values that the computer can manipulate. The reported results are an average of at least 70 counts. The area fraction and particles sizes were measured and for a random distribution of particles the volume fraction were supposed to be equal to the area fraction.

3. Results and discussion

During the solidification of AA3xxx alloys most of the Mn content exist in the solid solution, which results in the supersaturation of the solid solution. During heat treatment, the supersaturated solid solution will be decomposed by the precipitation of dispersoids. It is also known that the electrical conductivity of the alloy has a linear relationship with the reciprocal of the concentrations of alloying elements in solid solution [11].

The variation of electrical conductivity, uniform, post uniform and total elongations as a function of homogenization temperature are shown in Fig. 1. As shown in this figure both ductility and conductivity increased with increasing temperature up to 540°C and decreased with the further increasing of temperature. It is also interesting to note the maximum conductivity, the minimum of the supersaturation and precipitation potential, coincides with the maximum ductility. More recently, it

was shown that the ductility of the homogenized sheets mainly affected by the grain size and roughness of the material [12]. It is also obvious electrical conductivity increases with increasing homogenization temperature mainly due to the precipitation of (AlMnFe with Si and Mg) dispersoids. The decrease of electrical conductivity after 540°C is due to the increase of solubility of Mn in the matrix. Consequently, homogenization decomposed the supersaturation of the roll-cast material up to 540°C and reduced the precipitation potential in the homogenized samples and this could have mainly controlled the precipitation and recrystallization interaction.

The process of recrystallization and the grain sizes in the homogenized and unhomogenized conditions can be influenced by the interaction of recrystallization and precipitation and the presence of a dispersion of second-phase particles in the deformed matrix [13–16]. The precipitation and its interaction with recrystallization have been precisely studied by means of differential scanning calorimetry [7–9]. DSC results for the homogenized and unhomogenized casts are shown in Fig. 2. The as-cast undeformed alloy shows a very broad exothermic reaction in both conditions. The DSC curves for the rolled specimen showed different trends, Fig. 3. The unhomogenized rolled specimens show two weak exothermic peaks and a wide strong peak. The observed peaks have been explained differently. The three DSC peaks obtained by Howe [9] for a cold rolled unhomogenized AA3003 alloy interpreted respectively of the beginning of precipitation, recovery and maximum rate of the recrystallization. In contrast, according to the precise investigations of Garcia-Cordovilla [7, 8], the

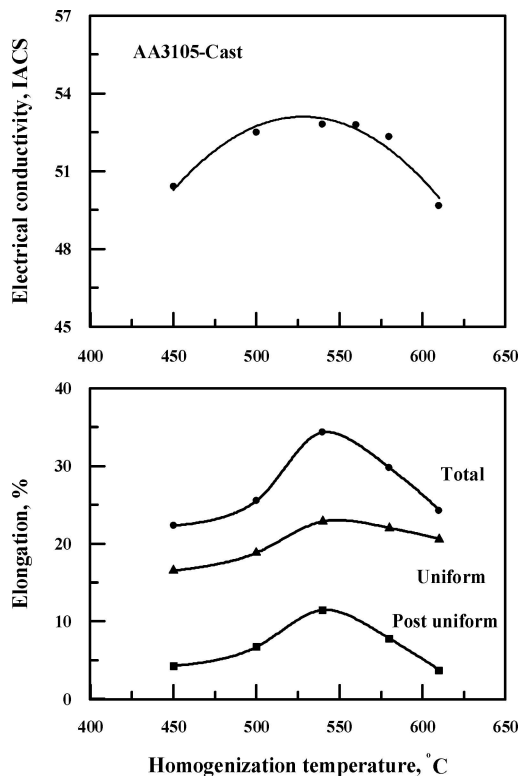


Figure 1 Variation of electrical conductivity of cast materials and uniform, post uniform and total elongations of those rolled and annealed at 350°C as a function of homogenization temperature.

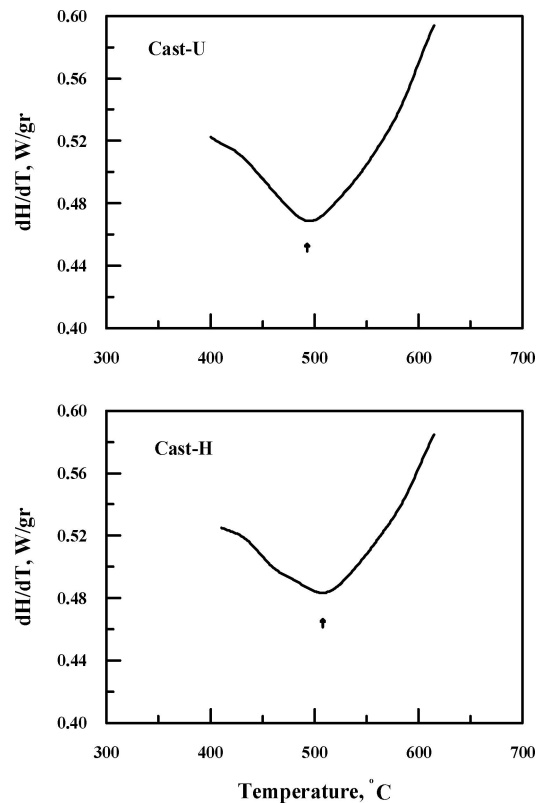


Figure 2 DSC curves for unhomogenized and homogenized cast materials.

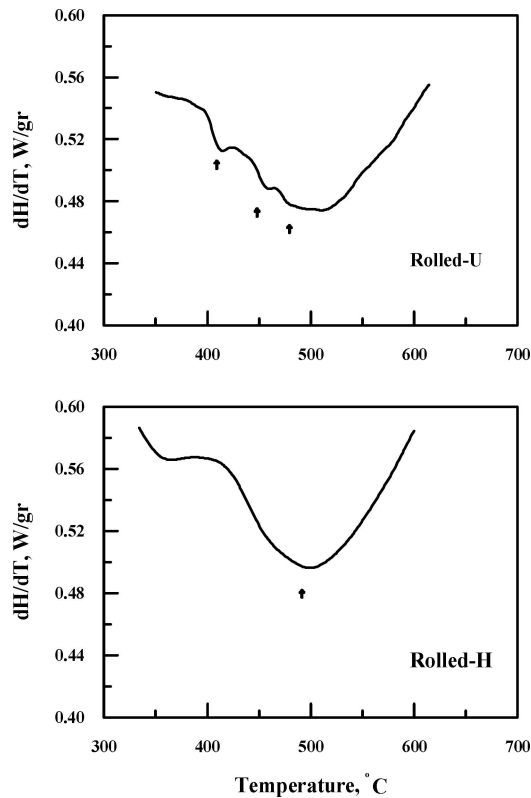


Figure 3 DSC curves for unhomogenized and homogenized rolled specimens.

three distinct peaks of the unhomogenized rolled specimen relate to low temperature precipitation, recrystallization and higher temperature precipitation. However, the similarity of the two wide exothermic peaks of the cast and rolled materials confirmed the last interpretation of the third peak.

The first and the second weak peaks are washed out in the homogenized specimen and only a wide exothermic peak remains. A single DSC peak in the homogenized Al-Mn alloy was detected [17], but it was not explained clearly. The exothermic peak of the homogenized sample is weaker than the unhomogenized one and is so wide. Therefore, this single peak can not reasonably describes restoration processes like recovery or recrystallization. Apparently, it relates to the weak precipitation phenomenon in the homogenized specimen.

The DSC results confirm the hypotheses that considers the effect of precipitation and recrystallization interaction; concurrent precipitation during annealing retards normal discontinuous recrystallization in the unhomogenized specimens, with finely dispersed second phase particles, and promotes continuous annealing as indicated by the softening curves, Fig. 4. On the other hand, homogenization causes normal discontinuous recrystallization and subsequent grain coarsening mainly due to the faded precipitation interaction and the coarsening of the second phase particles (Table I), Figs 5 and 6.

More recently, the transition from discontinuous to continuous recrystallization in some aluminum alloys have been investigated [18]. Continuous recrystallization was found to be promoted by a small initial grain

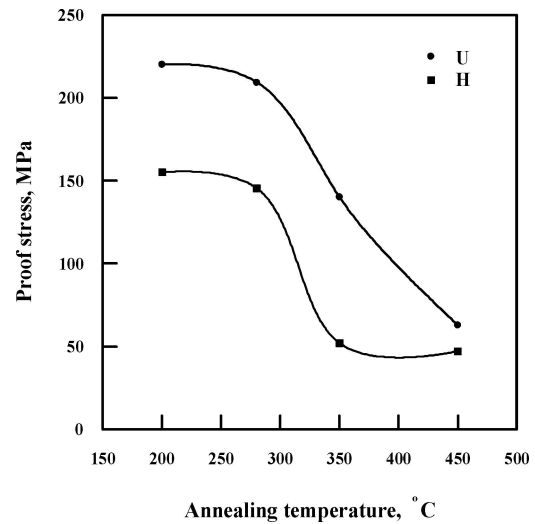


Figure 4 Variation of proof stress with annealing temperature for unhomogenized and homogenized sheets.

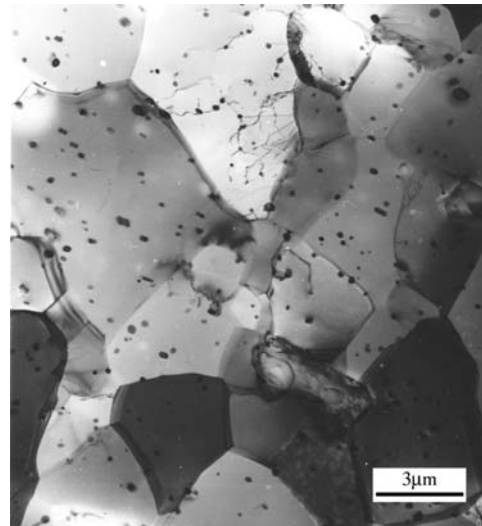


Figure 5 TEM micrograph of unhomogenized sheet following annealing at 450°C.

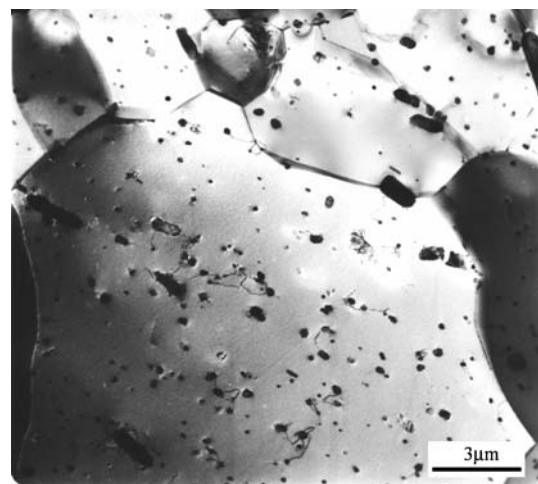


Figure 6 TEM micrograph of homogenized sheet following annealing at 450°C.

TABLE I Particle size, particle volume fraction and calculated grain sizes at 270°C annealing temperature

	Unhomogenized			Homogenized		
	d (μm)	F_v	D_z (μm)	d (μm)	F_v	D_z (μm)
Mean	0.240	0.030	5.330	0.420	0.037	7.570
Standard deviation	0.0640	0.0114	0.0527	0.0688	0.0086	0.0602
Standard error	0.0062	0.0011	0.0051	0.0080	0.0010	0.0070

TABLE II Particle size, particle volume fraction and calculated grain sizes at 350°C annealing temperature

	Unhomogenized			Homogenized		
	d (μm)	F_v	D_z (μm)	d (μm)	F_v	D_z (μm)
Mean	0.380	0.040	7.200	0.640	0.042	10.160
Standard deviation	0.1314	0.0144	0.1170	0.1604	0.0093	0.1511
Standard error	0.0137	0.0015	0.0122	0.0173	0.0010	0.0163

TABLE III Particle size, particle volume fraction and calculated grain sizes at 450°C annealing temperature

	Unhomogenized			Homogenized		
	d (μm)	F_v	D_z (μm)	d (μm)	F_v	D_z (μm)
Mean	0.240	0.030	5.330	0.420	0.037	7.570
Standard deviation	0.0640	0.0114	0.0527	0.0688	0.0086	0.0602
Standard error	0.0062	0.0011	0.0051	0.0080	0.0010	0.0070

size, large second-phase particles ($\geq 1 \mu\text{m}$) and large strains. In agreement with this investigation it is concluded larger initial grain size resulted from homogenization treatment should be one of the main cause of discontinuous recrystallization in the homogenized sheets. However, it is believed the presence of small particles and the interaction of precipitation and recrystallization in the unhomogenized sheets play important roles in discontinuous recrystallization. This mechanism is viewed as the pinning of subboundaries due to small particles at low annealing temperatures and their subsequent coarsening at higher temperature, enabling subgrain growth to occur via the migration of low- and high-angle boundaries [19, 20]. Obviously, the particle coarsening resulted from homogenization treatment discards this mechanism.

The material contains a distribution of both large and small particles ranges between 0.2 and 0.8 μm . Based on the image analysis data (Table I) the pinning forces due to the particles were calculated using the Zener pinning equation for a random distribution of spherical particles

$$P_Z = \frac{3F_v\gamma_B}{2r} \quad (1)$$

where F_v is the particle volume fraction, r the particle radius and γ_B the grain boundary energy. For aluminum, taking the energy of a high-angle grain boundary to be 0.625 J/m² [19], the pinning force exerted at each annealing temperature was calculated. If the Zener pinning force is plotted as a function of anneal-

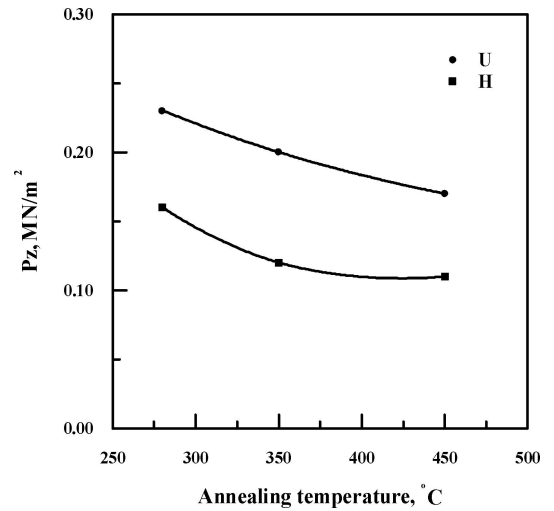


Figure 7 Graph showing the relationship between Zener pinning force and annealing temperature.

ing temperature (Fig. 7) it is apparent that the pinning force is smaller for the homogenized condition resulted in greater grain sizes in the homogenized sheets. The limiting grain sizes at different annealing temperatures were calculated using the Zener limit equation [6]

$$D_Z = k \left(\frac{r}{F_v} \right), \quad (2)$$

where, F_v is the particle volume fraction, r the particle radius and $k = \frac{4}{3}$ [19], shown in Tables I to III. It is

obvious the grain sizes is approximately one and half times in the homogenized conditions.

4. Conclusions

Contemporary investigations of electrical conductivity, differential scanning calorimetry and transmission electron microscopy confirmed that supersaturation decomposition and particle coarsening caused by homogenization treatment could affect the recrystallization and the precipitation during annealing of the Al-Mn-Mg sheets. It is believed that the homogenization condition which provide maximum ductility in the subsequently rolled sheets involves the lowest supersaturation, the highest electrical conductivity. This is mainly due to the effect of homogenization on the elimination of the recrystallization and precipitation interaction during annealing.

The grain coarsening effect, which is in turn a result of lower supersaturation and lower Zener pinning force in homogenized sheets annealed at high temperatures, encourages the surface roughening which can adversely affect the ductility of the material in this condition.

References

1. H. HERO and S. E. NAESS, *Metals Techn.* (1979) 245.
2. Y. KWAG Y and J.G. MORRIS, *Mater. Sci. Eng.* **77** (1986) 59.

3. E. NES, *Acta Metall.* **24** (1976) 391.
4. F.J. HUMPHREYS, *ibid.* **25** (1977) 1323.
5. P. R. MOULD and P. COTTERIL, *J. Mater. Sci.* **2** (1967) 241.
6. N. HANSEN and B. BAY, *ibid.* **7** (1972) 1351.
7. C. GARCIA-CORDOVILLA and E. LOUIS, *Metall Trans.* **15A** (1984) 389.
8. *Idem.*, *J. Mater. Sci.* **21** (1986) 971.
9. J. M. HOWE, *Metall Trans.* **17A** (1986) 593.
10. E. LOUIS and C. GARCIA-CORDOVILLA, *ibid.* **19** (1984) 689.
11. Y. J. LI and L. ARNBERG, *Acta Mater.* **51** (2003) 3415.
12. M. AGHAIE-KHAFRI, *J. Mater. Sci.* **39** (2004) 6467.
13. P. FURRER, N.A. RHEINFOLL and H. WARLIMONT, *Aluminium* **54** (1987) 135.
14. J. G. MORRIS and B. J. DUGGAN, *Metal Sci.* (1978) 1.
15. D. J. LLOYD, *ibid.* (1982) 304.
16. S. BENUM S and E. NES, *Acta Mater.* **45** (1997) 4953.
17. E. LOUIS and C. GARCIA-CORDOVILLA, in Proceedings of the 8th International Light Metals Congress, Leoben-Viena (Aluminium-Verlag GmbH, 1987) p. 452.
18. H. JAZAERI and F. J. HUMPHREYS, *Acta Mater.* **52** (2004) 3251.
19. R. K. DAVIES, V. RANDLE and G. J. MARSHALL, *ibid.* **46** (1998) 6021.
20. M. AGHAIE-KHAFRI and R. MAHMUDI, *Aluminum.* **74** (1998) 753.

Received 31 August

and accepted 22 November 2004